Journal of Constructional Steel Research 90 (2013) 253–264

Contents lists available at ScienceDirect

Journal of Constructional Steel Research

Optimal design of passive viscous damping systems for buildings under seismic excitation

Carlos A. Martínez, Oscar Curadelli *, María E. Compagnoni

Engineering Faculty, National University of Cuyo, CONICET, Mendoza, Argentina

ARTICLE INFO

Article history:
Received 24 April 2013
Accepted 6 August 2013
Available online xxxx

Keywords:
Optimal damper placement
Passive control
Viscous damper
Stochastic analysis

ABSTRACT

Nowadays, it is known that through the use of energy dissipation devices, the seismic performance of buildings can be improved. However, for efficiency and structural safety, the locations and sizes of these devices need to be properly defined. In this work, a procedure to optimally define the damping coefficients of added linear viscous dampers to meet an expected level of performance on buildings under seismic excitation is proposed. The performance criterion is expressed in terms of a maximum interstory drift, which is one of the most important limitations provided by the seismic design codes. For a given level of performance, the effectiveness of the damper distribution obtained by means of different objective functions is also assessed. Knowing that the main contribution to the total uncertainty is due to the excitation and with the aim of achieving robust results, the most appropriate approach to model the excitation is through a stationary stochastic process characterized by a power spectral density compatible with the response spectrum defined by the seismic design code. Accordingly, the structural response is obtained in the frequency domain. Through numerical examples, on planar and three-dimensional steel buildings with coupled lateral and torsional vibrations, the proposed procedure is verified.

1. Introduction

It is well known that, in order to reduce the structural response, external energy dissipation devices may be advantageously used. The effectiveness of these systems depends on, the damping capacity, as well as the placement of dampers into the structure. In view of these considerations, optimum design studies on energy dissipation systems have been of great interest, principally in earthquake engineering over the last two decades. In scientific literature, there are numerous studies related to optimal placement of dampers, mainly with viscous and viscoelastic devices, installed in shear type buildings.

Gluck et al. [1] suggested a method for the design of supplemental dampers and stiffness, based on optimal control theory, which minimizes a performance cost function, under the assumption of white-noise input. Takewaki [2] proposed a systematic algorithm for finding the optimal damper placement that minimizes the sum of amplitudes of the transfer functions of each interstory drift, evaluated at the undamped fundamental natural frequency of the structure subject to a constraint on the total added damping. Since the methodology was based on the amplitude of a transfer function, the characteristics of input motions were not considered. Wu et al. [3] investigated the optimal damper placement for three-dimensional structures taking into account translational and torsional responses. The authors demonstrated that the placement of a limited number of devices may have a significant effect on the level of response reduction. Through the Kanai–Tajimi filtered white-noise, the effect of ground motion characteristics was also examined. The results showed that the optimal placement is relatively dependent on the excitation. Takewaki and Yoshitomi [4] studied the effects of support stiffness on the optimal placement of viscous dampers and concluded that the support-member stiffness affects greatly the optimal damper positioning and the level of response reduction. Takewaki [5] described an original steepest direction search algorithm applied to the problem of optimal damper placement in structures subjected to critical excitation. With an algorithm similar to that introduced by Takewaki [5], Takewaki [6] presented an optimal damper placement approach to minimize the dynamic compliance transfer function of a planar building frame. Similar approach but using the transfer function amplitude of the base shear force evaluated at the undamped fundamental natural frequency of the structure was proposed by Aydin et al. [7]. Takewaki [8] developed a method for stiffness–damping simultaneous optimization of a structural system. A study on the optimal distribution of stiffness and damping using a generalized objective function was presented by Cimellaro [9]. In this work, the transfer function norms of the interstory relative displacement, absolute acceleration and base shear were evaluated at the fundamental natural frequency, and their amplitudes were minimized subject to a total stiffness and damping constraints. To demonstrate the validity of the methodology, dynamic response analysis was performed in time domain using an ensemble of 25 ground motion records.

To solve the optimal damper distribution problem, Singh and Moreschi [10] used a gradient-based optimization. Later, Singh and Moreschi [11] presented a study using genetic algorithm for

* Corresponding author at: Facultad de Ingeniería. Centro Universitario, Parque Gral. San Martín, 5500 Mendoza, Argentina. Tel.: +54 261 4135000 2195; fax: +54 261 4380120.
E-mail address: ocuradelli@fing.uncu.edu.ar (O. Curadelli).

0143-974X/$ – see front matter © 2013 Elsevier Ltd. All rights reserved.
http://dx.doi.org/10.1016/j.jcsr.2013.08.005

finding the optimal size and placement of viscous and viscoelastic dissipation devices required to achieve a required level of performance in different types of structures. A spectral density function of the type of Kanai–Tajimi was used to model the earthquake ground motion. An integrated optimum design of a viscoelastically damped structural system was described by Park et al. [12] in which, the optimization criterion was defined through a life-cycle cost function that takes into account the initial construction cost, and a probabilistic damage cost estimated over its lifetime. To find the optimum parameters, a genetic algorithm was implemented as a numerical searching technique. They conclude that increasing the amount of viscoelastic dampers is more efficient than increasing structural stiffness, especially with stiff soil conditions. Levy and Lavan [13] presented a method for optimal viscous damper design applied to linear and non-linear frame structures subjected to an ensemble of realistic ground motion records. Optimality criteria are formulated based on fully stressed characteristics of the optimal solution, and a simple analysis/redesign procedure is proposed for attaining optimal designs. García et al. [14] presented a theoretical and experimental investigation that deals with the torsional balance of elastic asymmetric structures through viscoelastic dampers. Results demonstrate that VE dampers are very effective in controlling lateral–torsional coupling of torsionally flexible as well as stiff structures. The devices are placed in such a way that, the empirical center of balance (point belongs to building plan where translations and rotations are statistically uncorrelated [15]) coincides with the geometrical center of the building plan.

Aydin and Boduroglu [16] presented a study comparing two rehabilitation techniques, energy dissipation through viscous dampers and stiffening by means of optimal placement of X steel diagonal braces. A book published in 2009 by Takewaki [17] shows a state-of-the-art on optimal performance-based design of buildings under seismic excitation provided with passive dampers. Aydin [18], developed a method to optimize the size and location of added viscous dampers based on base moment transfer function in planar steel frames. Different optimization techniques based on top displacement, top absolute acceleration and base shear are also compared. A recent work which compares the structural performance achieved by different techniques for optimal viscous damper placement by means of non-linear time history analyses was presented by Whittle et al. [19].

While many works deal with optimal damper distribution, only a few of them explicitly define the total added damping (damping capacity) of the energy dissipation system to achieve a required seismic performance.

A procedure to optimally define the damping coefficients of added viscous dampers to meet an expected level of performance on buildings under seismic excitation is proposed. The performance criterion is expressed in terms of a maximum interstory drift, which is one of the most important limitations provided by the seismic design codes. In order to assess the effectiveness of the damper distribution, for a given level of performance, different optimization strategies are addressed. The excitation is modeled as a stationary stochastic process characterized by a power spectral density compatible with the response spectrum defined by the seismic design code and the analysis is performed in the frequency domain.

Through numerical examples, on planar and three-dimensional steel buildings with coupled lateral and torsional effects, the proposed methodology is verified.

2. Model of earthquake excitation

Studies on dissipation systems' efficiency and influence of the excitation characteristics are carried out in time domain by Monte Carlo simulation using a sufficient number of deterministic artificially generated records [20]. However, in optimization problems with high computational cost due to numerous iterations, an alternative simple method is required. Stochastic analysis, conducted in frequency domain, is an attractive method in which, a power spectral density function (PSDF), rather than a collection of time histories, can be used for modeling the excitation.

2.1. Derivation of design spectrum compatible power spectral density function

It is known that earthquake excitation is inherently random, however, if the evolution of the frequency content with time can be neglected, the input ground motion can be characterized by a power spectral density function (PSDF). In this study the earthquake excitation is assumed as a stationary Gaussian random process $\ddot{x}_g(t)$ with zero mean represented by means of a design spectrum compatible PSDF. Following the methodology developed by Vanmarcke [21] cited in the work conducted by Giaralis and Spanos [22], the design spectrum compatible PSDF can be approximated by the following recursive equation:

$$G\left(\omega_j\right) = \frac{4\xi}{\omega_j\pi - 4\xi\omega_{j-1}}\left(\frac{S_a^2\left(\omega_j,\xi\right)}{\eta_j^2\left(\omega_j,\xi\right)} - \Delta\omega\sum_{k=1}^{j-1} G(\omega_k)\right) \quad \omega_j > \omega_0 \tag{1}$$

in which $G(\omega_j)$ and $S_a(\omega_j,\xi)$ are the one-sided PSDF and the median pseudo-acceleration response spectrum at a specific frequency ω_j, respectively, and $\xi = 0.05$ is the assumed damping ratio; $\Delta\omega$ is the frequency step in which the frequency range was discretized; the peak factor η_j is calculated by Eq. (2) and it represents the factor by which the root mean square (rms) value of the response of a SDOF oscillator must be multiplied to predict the level S_a below by which the peak response of the oscillator will remain, with probability p, throughout the duration of the input process T_s. Herein, the following approximated semi-empirical formula for the calculation of the peak factor is adopted, which is known to be reasonably reliable for earthquake engineering applications (Vanmarcke [21]):

$$\eta_j = \sqrt{2\ln\left\{2\upsilon_j\left[1-\exp\left(-q_j^{1.2}\sqrt{\pi\ln\left(2\upsilon_j\right)}\right)\right]\right\}} \tag{2}$$

in which

$$\upsilon_j = \frac{T_s}{2\pi}\omega_j(-\ln p)^{-1} \tag{3}$$

and

$$q_j = \sqrt{1-\frac{1}{1-\xi^2}\left(1-\frac{2}{\pi}\tan^{-1}\frac{\xi}{\sqrt{1-\xi^2}}\right)} \tag{4}$$

being Eqs. (3) and (4) close form expressions derived for a white noise PSDF which has to be a priori assumed without knowledge of $G(\omega_j)$ when the peak factor is calculated by Eq. (2); $T_s = 20$ sec. is the duration assumed for the underlying stationary process; $p = 0.5$ is an appropriate probability assumed for the purposes of this study; $\omega_0 = 0.36$ rad/s denotes the lowest bound of the existence domain of Eq. (3) for a PSDF and T_s a priori assumed [22].

The power spectrum density estimation obtained by Eq. (1) can be improved via the following iterative scheme [22]:

$$G^{i+1}\left(\omega_j\right) = G^i\left(\omega_j\right)\left[\frac{S_a^t\left(\omega_j,\xi\right)}{S_a^i\left(\omega_j,\xi\right)}\right]^2 \tag{5}$$

in which $S_a^t(\omega_j,\xi)$ and $S_a^i(\omega_j,\xi)$ are the target design spectrum and the associated design spectrum estimated in the ith iteration.

3. Evaluation of stochastic response

The equations governing the dynamic motion of the structure provided with viscous dampers subjected to earthquake excitation may be written in the matrix form as [6]:

$$\mathbf{M}\ddot{\mathbf{x}}(t) + (\mathbf{C} + \mathbf{C_v})\dot{\mathbf{x}}(t) + \mathbf{K}\mathbf{x}(t) = -\mathbf{M}\mathbf{r}\ddot{\mathbf{x}}_g(t) \tag{6}$$

where **M**, **K** and **C** are the mass, stiffness and the proportional damping matrices of size $n \times n$, respectively, the matrix of the added viscous damping is denoted by $\mathbf{C_v}$, **r** is the influence vector, $\ddot{\mathbf{x}}_g(t)$ is the horizontal acceleration of ground motion and $\mathbf{x}(t)$, $\dot{\mathbf{x}}(t)$ and $\mathbf{x}(t)$ are the generalized acceleration, velocity and displacement vectors, of size $n \times 1$ respectively, being n the number of degree of freedom. Eq. (6) can be written such as the following system of first-order differential equations:

$$\frac{d}{dt}\mathbf{y} = \mathbf{G}\mathbf{y} + \mathbf{w} \tag{7}$$

where **y** is the state vector

$$\mathbf{y} = \left\{ \mathbf{x}^T \quad \dot{\mathbf{x}}^T \right\}^T \tag{8}$$

G is the augmented system matrix

$$\mathbf{G} = \begin{bmatrix} [0] & [I] \\ -\mathbf{M}^{-1}\mathbf{K} & -\mathbf{M}^{-1}(\mathbf{C} + \mathbf{C_v}) \end{bmatrix} \tag{9}$$

and **w** is the excitation vector

$$\mathbf{w} = -\{ \{0\} \quad \{1\}\ddot{\mathbf{x}}_0 \}^T \tag{10}$$

where {0} and {1} denotes the null and unit vector, respectively, of size $1 \times n$; [0] and [I] denotes the null and identity matrix, respectively, of size $n \times n$; $\mathbf{M}^{-1}$ is the inverse of mass matrix **M**, and $\mathbf{x}_0(t)$ denotes the ground motion assumed as a zero-mean white noise random process with a PSDF of constant intensity, S_0.Let the covariance matrix of **y** be **S** with

$$S_{ij} = E\left[y_i y_j\right] \tag{11}$$

in which E[.] is the expectation operator and y_i is the ith element of vector **y**.

It can be shown [20] that for a zero-mean white noise random process, **S** satisfies the following differential equation:

$$\frac{d}{dt}\mathbf{S} = \mathbf{G}\mathbf{S}^T + \mathbf{S}\mathbf{G}^T + \mathbf{D} \tag{12}$$

in which **D** is the covariance matrix between the state and excitation vectors and $D_{ij} = 0$ except that $D_{2n,2n} = 2\pi\, S_0$,.

As the excitation is assumed stationary, **D** is time independent, then, the stationary solution of Eq. (12) can be obtained by solving the

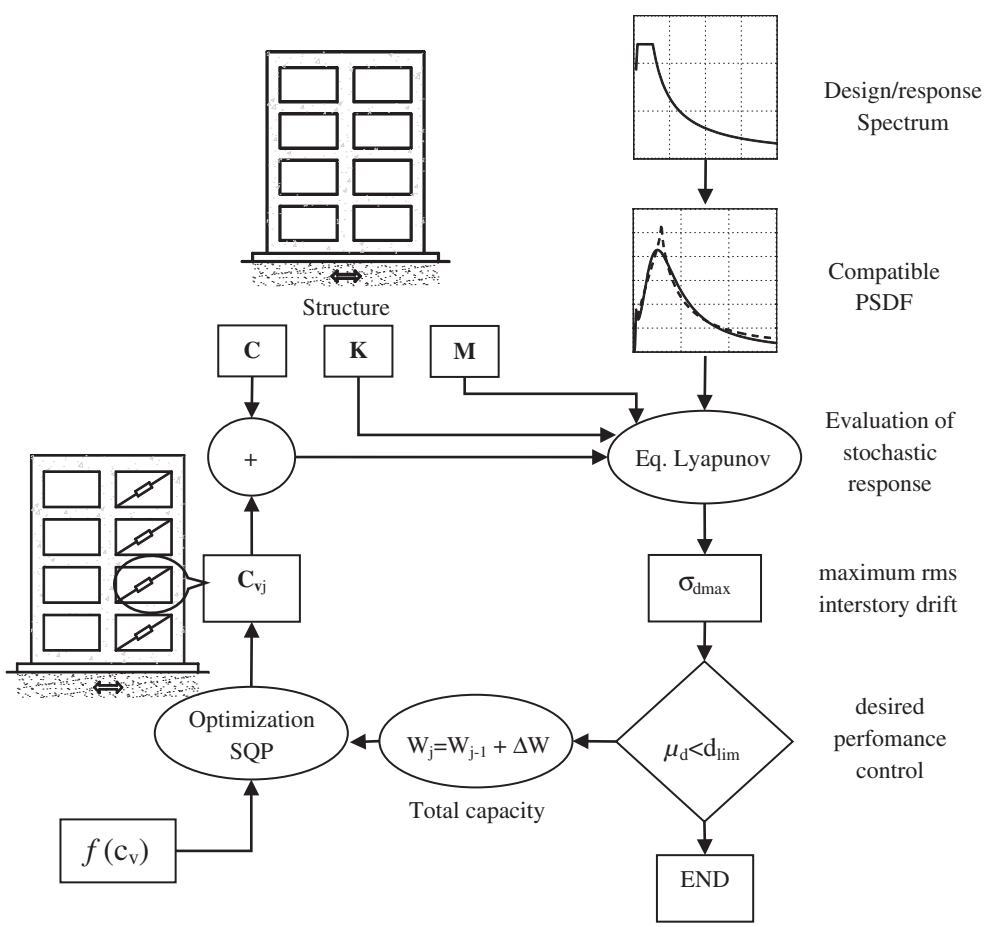

Fig 1. Flowchart of the proposed methodology.

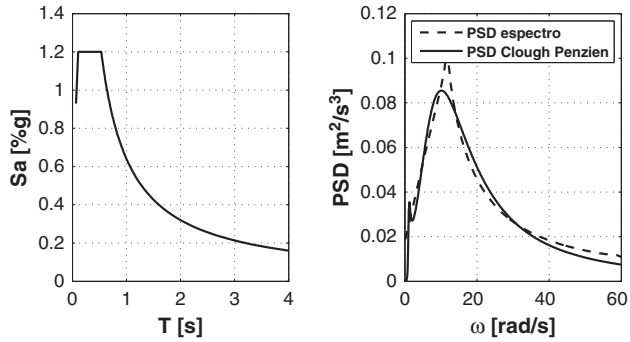

Fig. 2. Excitation characterized by: (a) UBC 97 design spectrum and (b) design spectrum compatible PSDF (dashed line) and Clough–Penzien approach (continuous line).

Lyapunov matrix equation

$$\mathbf{G}\mathbf{S}^T + \mathbf{S}\mathbf{G}^T + \mathbf{D} = 0. \tag{13}$$

Note that the previous stochastic response has been obtained for a white noise type excitation with constant PSDF; however, the PSDF obtained by Eq. (5) represents the stationary Gaussian random process, $x_g(t)$. This obstacle can be circumvented by filtering the white noise $x_0(t)$ through two linear filters as follows:

$$\ddot{x}_g(t) + 2\xi_g\omega_g\dot{x}_g(t) + \omega_g^2 x_g(t) = -\left(\ddot{x}_f(t) + x_0(t)\right), \tag{14}$$

$$\ddot{x}_f(t) + 2\xi_f\omega_f\dot{x}_f(t) + \omega_f^2 x_f(t) = -\ddot{x}_0(t) \tag{15}$$

in which ω_g, ξ_g, ω_f and ξ_f are the ground filter parameters. Eqs. (14) and (15) lead to the Clough and Penzien stationary PSDF [23]

$$G_{CP}\left(\omega_j\right) = S_0\left(\frac{1+4\xi_g^2\left(\omega_j/\omega_g\right)^2}{\left[1-\left(\omega_j/\omega_g\right)^2\right]^2+4\xi_g^2\left(\omega_j/\omega_g\right)^2}\right) \times \left(\frac{\left(\omega_j/\omega_f\right)^4}{\left[1-\left(\omega_j/\omega_f\right)^2\right]^2+4\xi_f^2\left(\omega_j/\omega_f\right)^2}\right). \tag{16}$$

Thus, to make compatible the PSDFs given by Eqs. (5) and (16), the filter parameters are estimated by fitting both functions.

On the basis of the above considerations, the stochastic structural response is obtained by solving Eq. (13) in which, the state vector, **y**, the augmented system matrix, **G**, and excitation vector, **w**, can be rewritten as follow:

$$\mathbf{y} = \left\{\mathbf{x}^T \quad \dot{\mathbf{x}}^T \quad x_f \quad \dot{x}_f \quad x_g \quad \dot{x}_g\right\}^T \tag{17}$$

$$\mathbf{G} = \begin{bmatrix} [0] & [I] & \{0\}^T & \{0\}^T & \{0\}^T & \{0\}^T \\ -\mathbf{M}^{-1}\mathbf{K} & -\mathbf{M}^{-1}(\mathbf{C}+\mathbf{C_v}) & -\{1\}^T\omega_f^2 & -\{1\}^T 2\xi_f\omega_f & \{1\}^T\omega_g^2 & \{1\}^T 2\xi_g\omega_g \\ \{0\} & \{0\} & 0 & 1 & 0 & 0 \\ \{0\} & \{0\} & -\omega_f^2 & -2\xi_f\omega_f & \omega_g^2 & 2\xi_g\omega_g \\ \{0\} & \{0\} & 0 & 0 & 0 & 1 \\ \{0\} & \{0\} & 0 & 0 & -\omega_g^2 & -2\xi_g\omega_g \end{bmatrix} \tag{18}$$

$$\mathbf{w} = \left\{\ \{0\} \quad \{0\} \quad 0 \quad 0 \quad 0 \quad -\ddot{x}_0\ \right\}^T \tag{19}$$

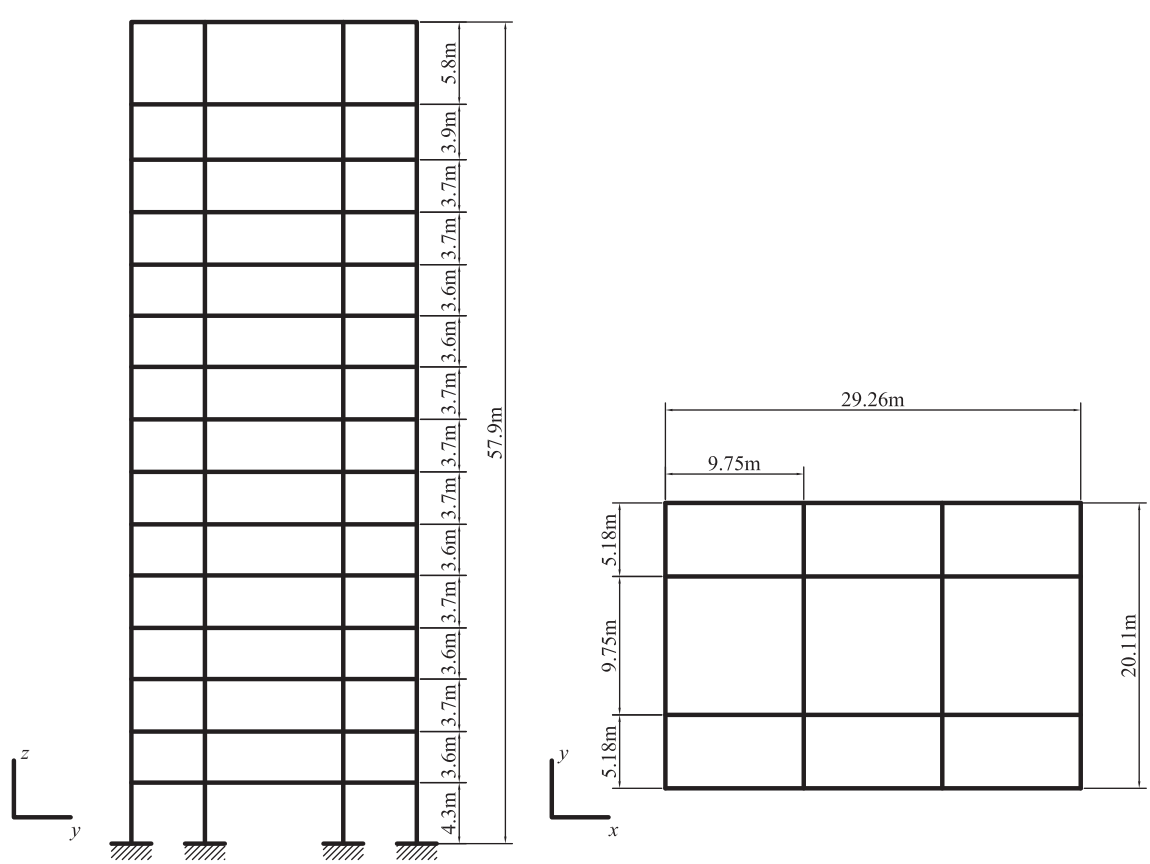

Fig. 3. Steel structure (Example 1) [30].

Table 1
Example 1: Model properties.

Story	Mass per floor [10^6 kg]	Stiffness [10^8 N/m]
1	0.2464	4.905
2	0.3986	4.905
3	0.3932	4.905
4	0.3932	4.4145
5	0.3905	4.4145
6	0.3905	4.4145
7	0.3905	4.1202
8	0.3905	4.1202
9	0.3905	3.924
10	0.3905	3.924
11	0.3905	3.924
12	0.3905	3.924
13	0.3905	3.7278
14	0.5844	3.5316
15	0.3624	2.7468

and the elements of the covariance matrix $\mathbf{D}$ of size $2n+4 \times 2n+4$ are $D_{ij}=0$ except that $D_{2n+4,2n+4}=2\pi S_0$.

4. Optimal placement of viscous dampers

The challenge for the problem of optimal viscous damper placement is to find, in every possible location, the damping coefficient c_{vi} which minimize/maximize a given objective function f. Then, the optimization problem is stated as follows:

$$\min_{\mathbf{c_v}}/\max f(\mathbf{c_v}) \tag{20}$$

subject to the constraints on the total added damping and on each damping coefficient given by:

$$\sum_{i=1}^{n_d} c_{v_i} = \overline{W} \tag{21}$$

$$0 \le c_{v_i} \le \overline{W} \quad i = 1 \ldots n_d \tag{22}$$

where $\overline{W}$ is the damping capacity needed to achieve the required structural performance and n_d is the number of added dampers.

4.1. Objective function

Different objective functions can be chosen depending on the required design objective. With the aim of assessing different strategies, in this study, the following objective functions are presented:

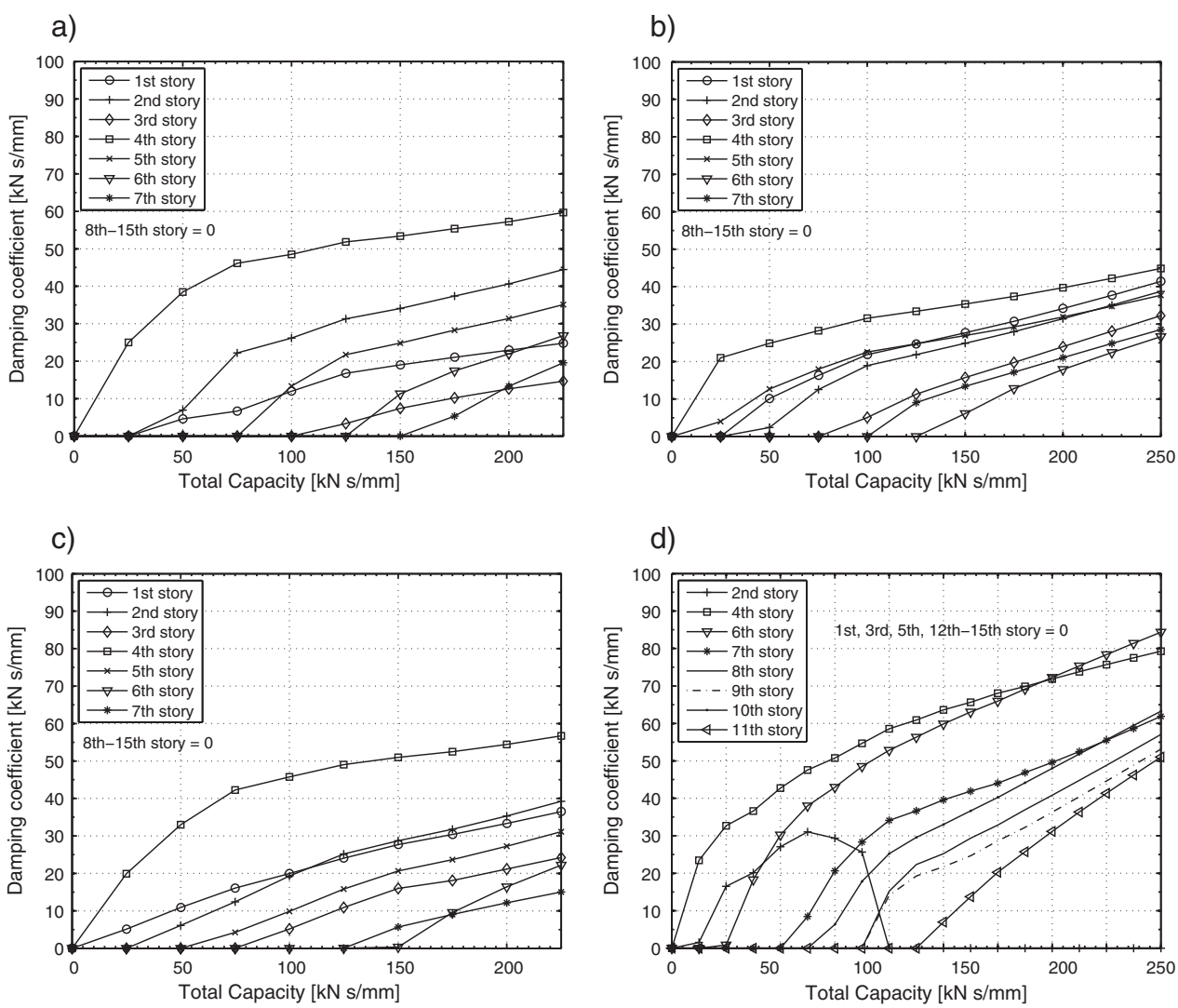

Fig. 4. Damping coefficient vs. damping capacity. Objective function: (a) max drift. (b) Top displacement. (c) Sum of maximum drift and base shear force. (d) Dissipated energy.

4.1.1. Minimization of maximum drift

This strategy seeks to reduce the structural dynamic response through the control of maximum interstory drift. Based on this premise, the optimization problem may be formulated as follows: Find the vector of the damping coefficients $\mathbf{c_v} = \{c_{vi}\}$ of added dampers, which minimize the maximum root mean square (rms) value of interstory drifts of the structure. Thus, the objective function takes the form:

$$\underset{\mathbf{c_v}}{\text{minimize}}\ \sigma_{d\,\max} = \max\left(\sigma_{d_1}, \sigma_{d_2}, \ldots, \sigma_{d_n}\right) \tag{23}$$

where the vector of the rms values of interstory drifts $\boldsymbol{\sigma}_\mathbf{d} = \left\{\sigma_{d_1}, \sigma_{d_2}, \ldots, \sigma_{d_n}\right\}$ can be obtained as [24]:

$$\boldsymbol{\sigma}_\mathbf{d} = \text{diag}\left(\mathbf{TST}^T\right)^{1/2} \tag{24}$$

in which $\mathbf{T}$ is a constant matrix consisting of 1, −1 and 0 and $\mathbf{S}$ is obtained by solving Eq. (13).

4.1.2. Minimization of top displacement

The problem of optimal damper distribution based on the minimization of the top displacement may be formulated as follows: Find the vector of the damping coefficients $\mathbf{c_v} = \{c_{vi}\}$ of added dampers, which minimize the rms of the top displacement of the structure. Thus, the objective function can be expressed as

$$\underset{\mathbf{c_v}}{\text{minimize}}\ \sigma_{x_n} \tag{25}$$

where the root mean square value of top displacement σ_{x_n} is the square root of the n-th element in the diagonal of matrix $\mathbf{S}$, which corresponds to the top displacement degree of freedom.

4.1.3. Minimization of the sum of maximum drift and base shear force

Because interstory drift and top displacement are essential deformation parameters for seismic design, the minimization of both, is essential for determining optimal damper placement. However, the structural deformation reduction can be achieved by increasing the stiffness, which can lead to increase the base shear force. Therefore, both, interstory drift and base shear force should be considered in the optimization problem. Accordingly, the problem of optimal damper placement may be stated as the sum of the rms values of the maximum interstory drift and base shear force, both, relative to the values obtained on the original structure (without added dampers). Thus, the objective function takes the form:

$$\underset{\mathbf{c_v}}{\text{minimize}}\ \frac{\sigma_{d\,\max}}{\sigma_{d_0\,\max}} + \frac{\sigma_v}{\sigma_{v_0}} \tag{26}$$

where $\sigma_{d\ \max}$ is the maximum rms value of interstory drifts of the structure, σ_v is the rms value of the base shear force and the subscript 0 indicates values of the original structure.

The rms value of base shear force can be obtained as follows [24]

$$\sigma_v = \left(\mathbf{rKS_xK}^T\mathbf{r}^T + \mathbf{r}(\mathbf{C}+\mathbf{C_v})\mathbf{S}_{\dot{\mathbf{x}}}(\mathbf{C}+\mathbf{C_v})^T\mathbf{r}^T\right)^{1/2} \tag{27}$$

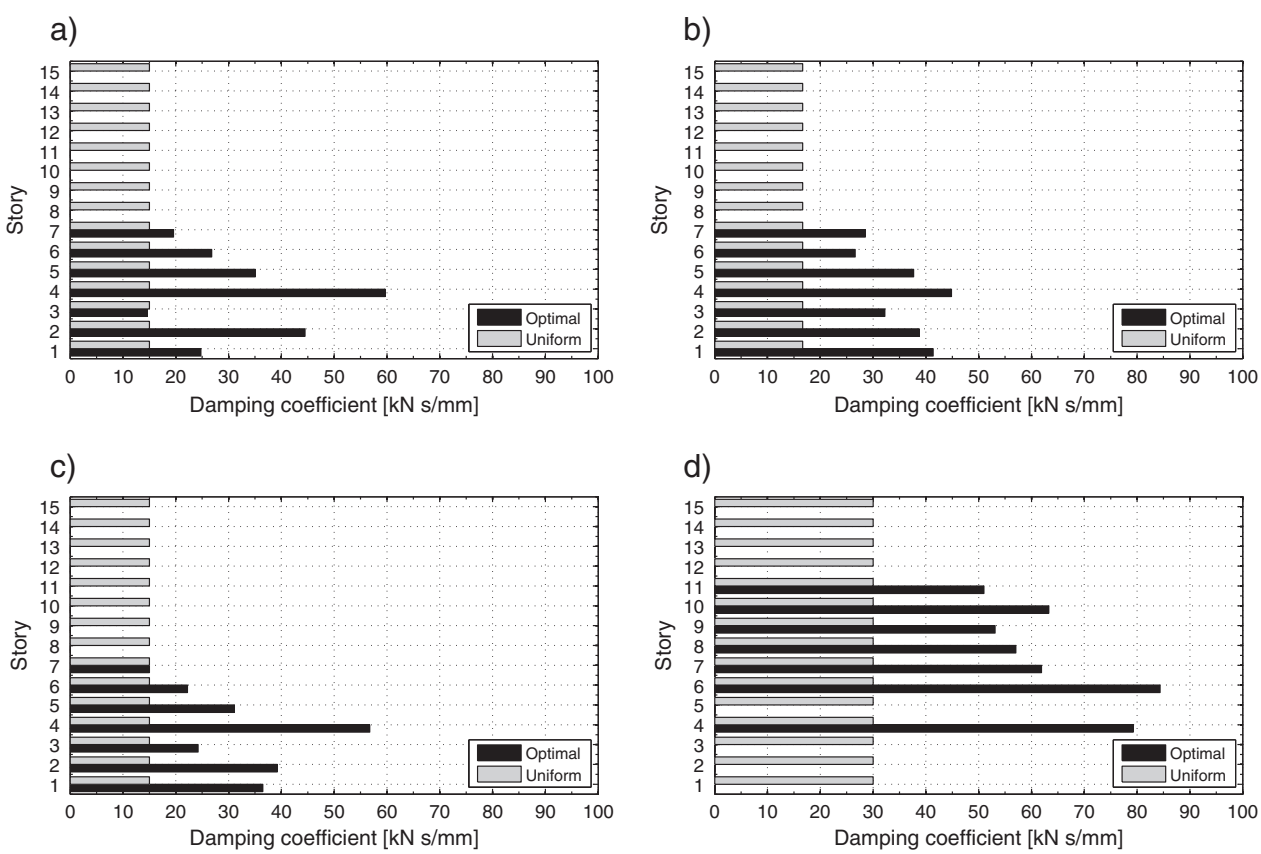

Fig. 5. Final damping coefficient for maximum story drift equal 1%. Objective function: (a) max drift. (b) Top displacement. (c) Sum of maximum drift and base shear force. (d) Dissipated energy.

Table 2
Objective functions efficiency (for a maximum interstory drift equal to 1%).

Objective function	Total damping capacity [kNs/mm]	Base shear force [10^3 kN]	Top displacement [m]	ξ [%]
Min (maximum drift)	220	7.674	0.1713	10.13
Min (top displacement)	240	7.332	0.1642	10.90
Min (max drift + base shear force)	220	7.589	0.1707	10.16
Max (dissipated energy)	450	7.119	0.1412	15.11
Uniform	380	7.007	0.1559	11.51

Table 3
Example 2: Floor mass and stiffness.

Story	Mass per floor		Stiffness	
	Translation [kg]	Rotational [10^7 kg m^2]	Longitudinal X [kN/m]	Transverse Y [kN/m]
1	358,000	5.5379	412,800	446,760
2	358,000	5.5379	412,800	446,760
3	358,000	5.5379	412,800	446,760
4	358,000	5.5379	412,800	446,760
5	358,000	5.5379	412,800	446,760
6	358,000	5.5379	412,800	446,760

where the sub-matrices of **S** are:

$$\mathbf{S_x} = \begin{bmatrix} S_{1,1} & S_{1,2} & \cdots & S_{1,n} \\ S_{2,1} & S_{2,2} & \cdots & S_{2,n} \\ \vdots & \vdots & \ddots & \vdots \\ S_{n,1} & S_{n,2} & \cdots & S_{n,n} \end{bmatrix} \text{ and } \mathbf{S_x} = \begin{bmatrix} S_{n+1,n+1} & S_{n+1,n+2} & \cdots & S_{n+1,2n} \\ S_{n+2,n+1} & S_{n+2,n+2} & \cdots & S_{n+2,2n} \\ \vdots & \vdots & \ddots & \vdots \\ S_{2n,n+1} & S_{2n,n+2} & \cdots & S_{2n,2n} \end{bmatrix}. \tag{28}$$

4.1.4. Maximization of dissipated energy

Another attractive strategy based on dissipated energy for optimal damper distribution may be formulated as: Find the vector of the damping coefficients $\mathbf{c_v} = \{c_{vi}\}$, which maximize the total dissipated energy through the dampers. Thus, the objective function is expressed as follows:

$$\underset{\mathbf{c_v}}{\text{maximize}}\ E_d \tag{29}$$

where E_d represents the total dissipated energy per cycle determined as:

$$E_d = \sum_{i=1}^{n_d} c_{v_i} \omega_1 \pi \Delta_i^2 \tag{30}$$

where Δ_i is the relative displacement amplitude of the cycle under consideration, n_d is the number of added dampers, c_{v_i} is the damping coefficient of the ith damper and ω_1 is the natural frequency of the structure. In this study Δ_i was assumed equal to the rms of the relative displacement $\sigma_{\Delta i}$ of each damper during the excitation motion. Then

$$E_d = \sum_{i=1}^{n_d} c_{v_i} \omega_1 \pi \sigma_{\Delta i}^2. \tag{31}$$

4.2. Required performance

Limitations on interstory drift are given by seismic design code provisions to control deformations and to prevent potential instabilities in both structural and non-structural elements. To define the minimum damping capacity of the dissipation system, the peak of the maximum interstory drift was adopted as performance criterion. In accordance with the provision of the IBC 2003 [25], for a typical steel shear structure, seismic use group III, the interstory drift limit is 0.010. Thus, an interstory drift limit equal to 0.010 will be used in the next examples as level of performance required for the dissipation system design.

For a given excitation, the mean peak of the maximum interstory drift can be calculated from the maximum root mean square value determined by Eq. (23) as follows (Der Kiureghian [26]):

$$\mu_{d\max} = p_f \sigma_{d\max} \tag{32}$$

$$p_f = \sqrt{2 \ln \nu_e \tau} + \frac{0.5775}{\sqrt{2 \ln \nu_e \tau}} \tag{33}$$

where $\mu_{d\max}$ is the mean peak of the maximum interstory drift, p_f is the peak factor, $\sigma_{d\max}$ (Eq. 23) is the standard deviation of the maximum interstory drift, ν_e is the modified mean zero-crossing rate, and τ is the time duration of the excitation. Der Kiureghian [26] derived a simple expression for ν_e from a SDOF subjected to white noise ground acceleration

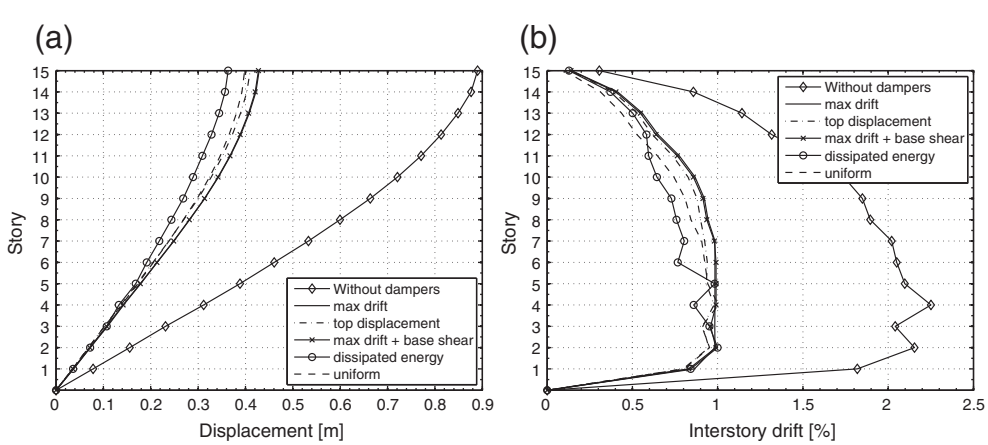

Fig. 6. Response for different objective functions. (a) Peak interstory drift. (b) Peak absolute displacements.

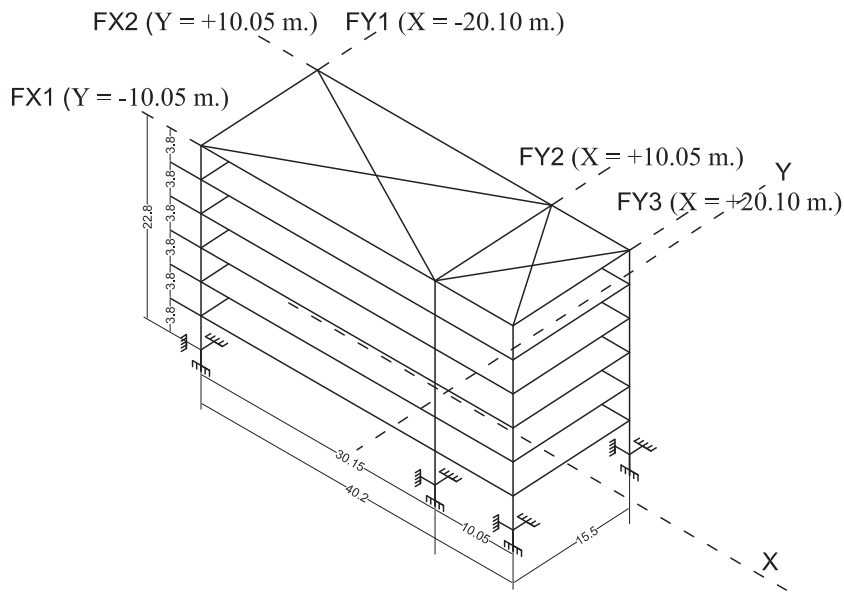

Fig. 7. 6-Story high steel frame building (Example 2).

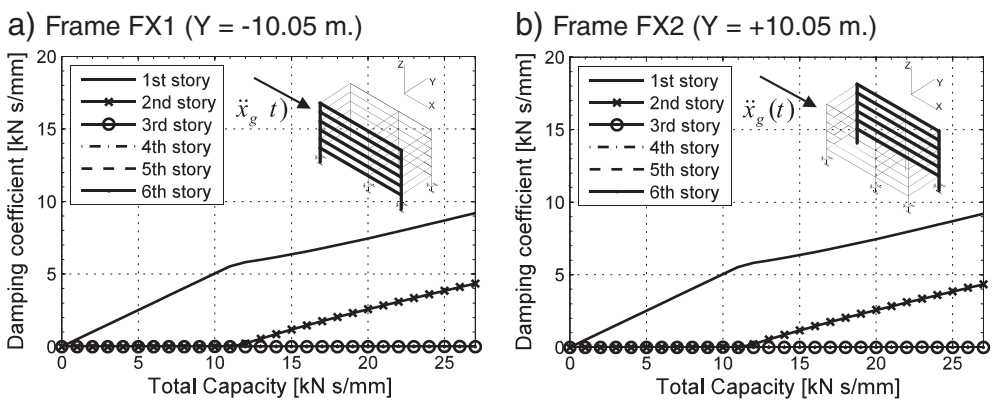

Fig. 8. Damping coefficient vs. damping capacity. Excitation: X direction.

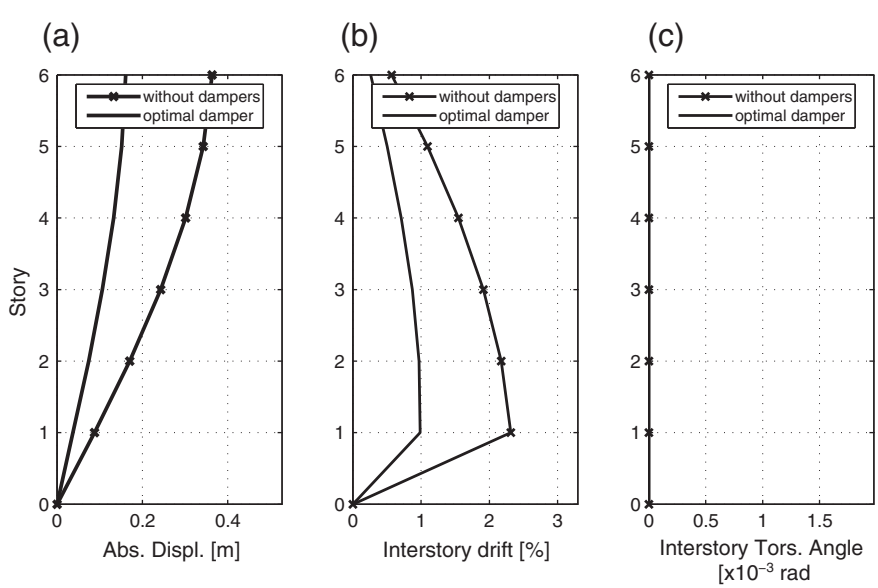

Fig. 9. Structural response. (a) Peak of absolute displacement. (b) Peak of interstory drift. (c) Peak of interstory torsional angle. Excitation: X direction.

given by:

$$\nu_e = \begin{cases} \left(1.90\xi^{0.15} - 0.73\right)\nu, & (\xi < 0.54) \\ \nu, & (\xi \geq 0.54) \end{cases} \tag{34}$$

where

$$\nu = \frac{\omega_1}{\pi} \tag{35}$$

in which ν is the zero-crossing rate of the response, and ω_1 and ξ are the natural frequency and the damping ratio of the SDOF structure, respectively. For multi-degree-of-freedom (MDOF) structures, the natural frequency and damping ratio of the fundamental vibration mode are used under the assumption that the fundamental mode dominates the dynamic response.

5. Optimization procedure

In this study, the Sequential Quadratic Programming (SQP) method [27,28] was chosen to solve the optimization problem stated by the objective function and constraint equations (Eqs. 20, 21 and 22). The proposed procedure, which includes the SQP algorithm, defines the damping coefficient c_{vi}, in every possible location sequentially, for gradually increasing damping capacity until the required performance is achieved. The procedure starts with the structure model without added dampers, i.e. $c_{vi} = 0$. Once the filter parameters have been determined, the stochastic response is evaluated by Eq. (13) (see Section 3). From Eq. (32), the peak of maximum interstory drift is calculated and then compared with the limitations provided by the seismic code (Section 4.2). If the required performance level is achieved, the procedure ends, else, the damping capacity $\overline{W}$ is increased by a damping step ΔW. Given ΔW, the optimal damping coefficients c_{vi} are determined through the SQP algorithm, considering the selected objective function. Then, the matrix of the added dampers $\mathbf{C_v}$ must be added to the damping matrix

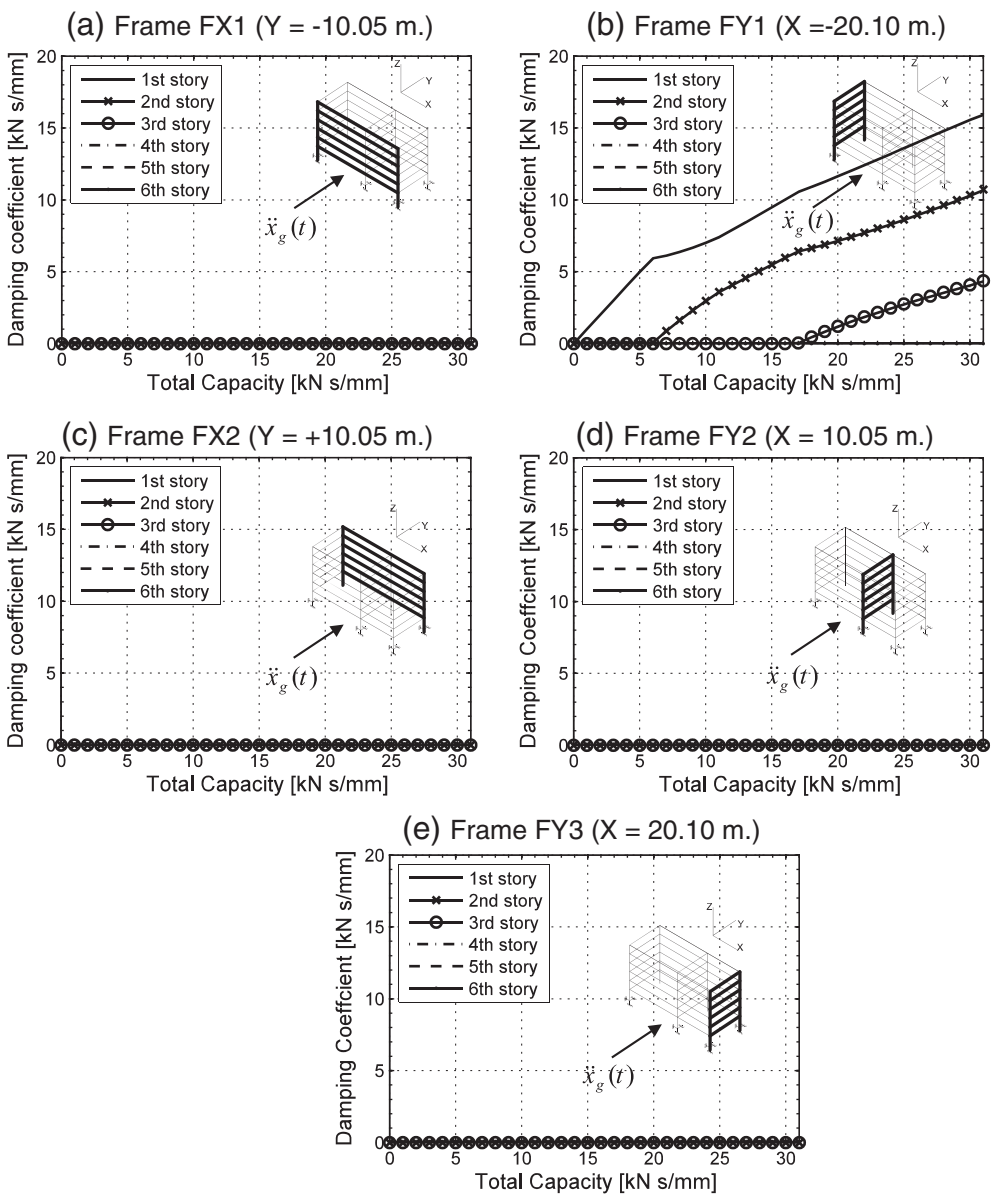

Fig. 10. Damping coefficient vs. damping capacity. Excitation: Y direction.

C of the original structure to reevaluate the stochastic response by solving Eq. (13). The procedure continues until the required performance is achieved. For clarity, in Fig. 1 the flowchart of the proposed methodology is shown.

6. Numerical examples

6.1. Excitation

In this study, the excitation was defined from the UBC 97 [29] response spectrum. Fig. 2(a) shows the UBC 97 pseudo-acceleration response spectrum for seismic zone 4, soil profile type S_B, and seismic source type A, with closest distance to known seismic source equal to 5 km. In Fig. 2(b) the corresponding compatible PSDF obtained by Eq. (5) (dashed line) and the Clough–Penzien approach (Eq. 16) (continuous line) are displayed.

6.2. Example 1: 15 story planar building frame

This example consists of four steel moment-resisting frames in each direction, 15-story high, in a building with two planes of symmetry [30]. Fig. 3 shows the geometric characteristics of the structure and the mass per floor and story stiffness on the z–y plane are indicated in Table 1. For low amplitude vibration, the fundamental period resulted equal to $T_1 = 1.89$ s. The internal damping was assumed equal to 2% of critical damping ratio.

Using the proposed methodology, the optimal damper placement for every objective function (Section 4.2) and increasing damping capacity is performed. Fig. 4(a)–(d) shows that different objective functions lead to similar damper distributions at each damping capacity, except for the maximum dissipated energy objective function.

The final distribution of added dampers that lead to the required level of performance (max story drift = 1%) for every objective function is presented in Fig. 5(a)–(d). For comparison purposes, the corresponding uniform distribution is also included. As can be seen in Fig. 5(a)–(c), the dampers are added in first seven stories, with damping capacities of 220, 240 and 220 kNs/mm for each of the respective objective functions. In the case of dissipated energy objective function, the optimization procedure indicates that the damping capacity of 450 kNs/mm should be distributed between 4th and 11th story, except in the 5th story (Fig. 5(d)).

While, similar performances in terms of maximum interstory drift, base shear force and top displacement have been achieved with all objective functions (see Table 2), the damping capacity required for the uniform distribution and dissipated energy is markedly different of the other objective functions. From Fig. 6(a) and (b), it is clear that although those two distributions lead to smaller absolute displacement at expense of higher damping, they display inefficiency in the maximum interstory drift control.

Because one of the most efficient objective function is the sum of the maximum interstory drift and base shear force, it will be used in the next example.

6.3. Example 2: 6 story 3D building with one direction eccentricity

In order to assess the lateral and torsional vibration control, a 6-story high steel frame building with one direction eccentricity is considered. The structure consists of three identical moment-resisting frames in Y direction and two in X direction. Principal properties are summarized in Table 3 and general dimensions are indicated in Fig. 7. The fundamental periods in both directions, for low amplitude vibration, are $T_{1x} = 0.77$ s and $T_{1y} = 0.76$ s. The internal damping was assumed equal to 2% of the critical.

The global stiffness and mass matrices for a coordinate system located in mass center are given by:

$$\mathbf{K} = \begin{bmatrix} \sum_i \mathbf{k}_{\mathbf{x}i} & 0 & -\sum_i \mathbf{k}_{\mathbf{x}i} Y_i \\ 0 & \sum_i \mathbf{k}_{\mathbf{y}i} & \sum_i \mathbf{k}_{\mathbf{y}i} X_i \\ -\sum_i \mathbf{k}_{\mathbf{x}i} Y_i & \sum_i \mathbf{k}_{\mathbf{y}i} X_i & \sum_i \left(\mathbf{k}_{\mathbf{x}i} Y_i^2 + \mathbf{k}_{\mathbf{y}i} X_i^2 \right) \end{bmatrix} \tag{36}$$

$$\mathbf{M} = \begin{bmatrix} \mathbf{M}_t & 0 & 0 \\ 0 & \mathbf{M}_t & 0 \\ 0 & 0 & \mathbf{M}_\theta \end{bmatrix} \tag{37}$$

where $\mathbf{M_t}$ and $\mathbf{M_\theta}$ are the translational mass and the mass moment of inertia diagonal matrices, respectively and the external added damper matrix is:

$$\mathbf{C_v} = \begin{bmatrix} \sum_i \mathbf{C}_{\mathbf{vx}_i} & 0 & -\sum_i \mathbf{C}_{\mathbf{vx}_i} Y_i \\ 0 & \sum_i \mathbf{C}_{\mathbf{vy}_i} & \sum_i \mathbf{C}_{\mathbf{vy}_i} X_i \\ -\sum_i \mathbf{C}_{\mathbf{vx}_i} Y_i & \sum_i \mathbf{C}_{\mathbf{vy}_i} X_i & \sum_i \left(\mathbf{C}_{\mathbf{vx}_i} Y_i^2 + \mathbf{C}_{\mathbf{vy}_i} X_i^2 \right) \end{bmatrix} \tag{38}$$

where i indicates the ith frame into the structure, $\mathbf{k}_{\mathbf{x/y}i}$ and $\mathbf{C}_{\mathbf{vx/y}_i}$ are the stiffness and damper matrix in X/Y direction of the ith frame, respectively; and X_i and Y_i represent the distances in X and Y direction of the ith frame to the mass center, respectively.

Using as objective function the maximum drift and base shear force and a maximum story drift equal to 1% as performance criteria, the optimization procedure is conducted.

Assuming that the excitation initially acts in X direction (structure without eccentricity), the optimal damper coefficients in each frame for increasing damping capacity and the structural response, in X direction, for a damping capacity of 27 kNs/mm are displayed in Figs. 8 and 9, respectively. Since, in this case there is no eccentricity, the total required damping has only been used to meet the allowed translational interstory drift of 1%. As expected, Fig. 8 shows that, the damping capacity is equally distributed among both frames located in the excitation direction. No

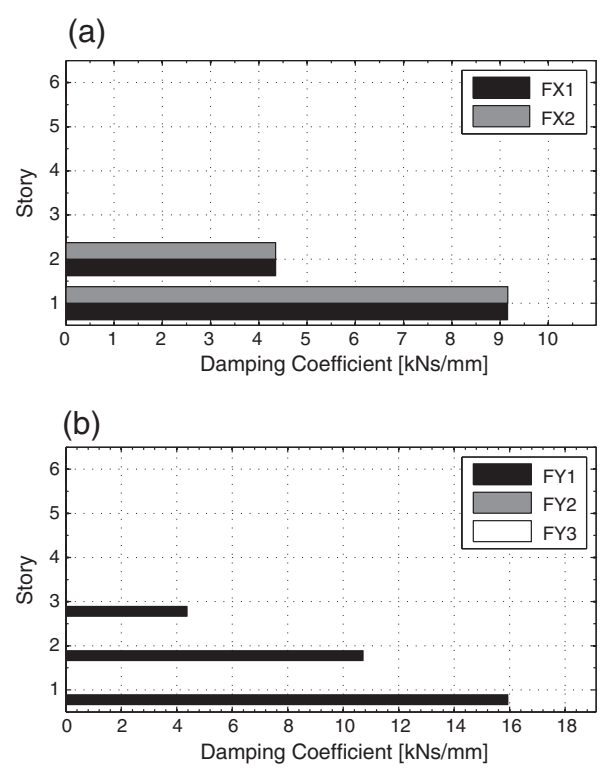

Fig. 11. Final damping coefficient for maximum drift equal 1%. (a) X direction frames. (b) Y direction frames.

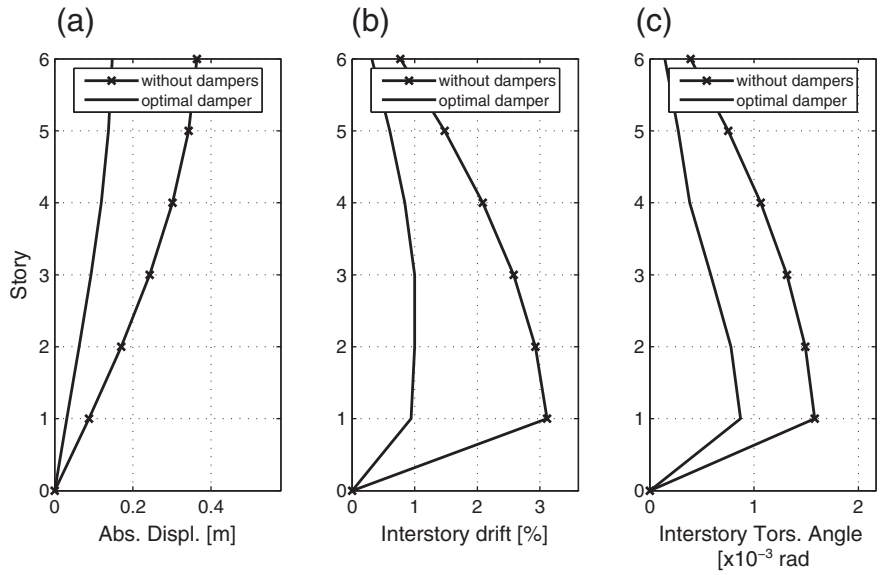

Fig. 12. Structural response. (a) Peak of absolute displacement. (b) Peak of interstory drift. (c) Peak of interstory torsional angle. Excitation: Y direction.

dampers are placed in frames oriented with Y direction. It can also be seen that the dampers are gradually installed at the first and second stories, which present greater drift (Fig. 9(b)).

With an installed damping capacity equal to 13.5 kNs/mm in each FXi frame, the analysis is now conducted with the same excitation acting in Y direction (eccentric structure). From Fig. 10 it is clear that, for achieving the required performance, the optimization procedure aims to reduce the stiffness eccentricity and the excessive drift adding dampers in the first three stories of the farthest frame (FY1).

Fig. 11 shows how the final damping capacity of 57 kNs/mm should be distributed per story and frame to achieve the performance criterion (max drift = 1%). The corresponding lateral and torsional structural response, in Y direction, is displayed in Fig. 12.

Because the system is linear, the same results had been obtained assuming the excitation in reverse order, initially in Y direction and then X direction.

7. Conclusions

From the present study it is worth mentioning the following issues:

- The proposed procedure allows optimally designing viscous energy dissipation systems in a computationally efficient way.
- The excitation modeled as a stationary stochastic process defined by a design spectrum compatible PSD, which characterizes the seismic excitation at the structure site, enabled to achieve a robust design of the dissipation system.
- The comparative study allowed inferring that similar seismic performance may be achieved in terms of interstory drift and base shear force using any of the objective functions studied, with the exception of the case of maximum dissipated energy through the dampers, which exhibited a low efficiency.
- The robustness of the optimization algorithm in addressing translational–torsional coupling problems was also confirmed.
- Results showed that for building structures with different stiffness distribution over the height, the devices should be placed where the greatest interstory drifts occur (usually on the first stories). Additionally, it is clear that the optimization procedure aims to correct the stiffness eccentricity, by placing the dampers in such a way to simultaneously minimize both, the torsional effects and the translational response.

Acknowledgments

The financial support of CONICET and National University of Cuyo is gratefully acknowledged.

References

[1] Gluck N, Reinhorn AM, Gluck J, Levy R. Design of supplemental dampers for control of structure. J Struct Eng ASCE 1996;122(12):1394–9.
[2] Takewaki I. Optimum damper placement for minimum transfer functions. Earthq Eng Struct Dyn 1997;26:1113–24.
[3] Wu B, Ou J-P, Soong TT. Optimal placement of energy dissipation devices for three-dimensional structures. Eng Struct 1997;19(2):113–25.
[4] Takewaki I, Yoshitomi S. Effects of support stiffnesses on optimal damper placement for a planar building frame. Struct Des Tall Build 1998;7:323–36.
[5] Takewaki I. Optimal damper placement for critical excitation. Probab Eng Mech 2000;15:317–25.
[6] Takewaki I. Optimum damper placement for planar building frames using transfer functions. Struct Multidiscip Optim 2000;20:280–7.
[7] Aydin E, Boduroglu MH, Guney D. Optimal damper distribution for seismic rehabilitation of planar building structures. Eng Struct 2007;29:176–85.
[8] Takewaki I. An approach to stiffness–damping simultaneous optimization. Comput Methods Appl Mech Eng 2000;189:641–50.
[9] Cimellaro GP. Simultaneous stiffness–damping optimization of structures with respect to acceleration displacement and base shear. Eng Struct 2007;29:2853–70.
[10] Singh MP, Moreschi LM. Optimum seismic response control with dampers. Earthq Eng Struct Dyn 2001;30:553–72.
[11] Singh MP, Moreschi LM. Optimal placement of dampers for passive response control. Earthq Eng Struct Dyn 2002;31:955–76.
[12] Park K-S, Koh H-M, Hahm D. Integrated optimum design of viscoelastically damped structural systems. Eng Struct 2004;26:581–91.
[13] Levy R, Lavan O. Fully stressed design of passive controllers in framed structures for seismic loadings. Struct Multidiscip Optim 2006;32(6):485–9.
[14] García M, de la Llera JC, Almazán JL. Torsional balance of plan asymmetric structures with viscoelastic dampers. Eng Struct 2007;29:914–32.
[15] De la Llera JC, Almazán JL, Vial IJ. Torsional balance of plan-asymmetric structures with frictional dampers: analytical results. Earthquake Eng Struct Dyn 2005;34:1089–108.
[16] Aydin E, Boduroglu MH. Optimal placement of steel diagonal braces for upgrading the seismic capacity of existing structures and its comparison with optimal dampers. J Constr Steel Res 2008;64:72–86.
[17] Takewaki I. Building control with passive dampers. Optimal performance-based design for earthquakes. Kioto University, Japan: John Wiley & Sons (Asia) Pte. Ltd.; 2009
[18] Aydin E. Optimal damper placement based on base moment in steel building frames. J Constr Steel Res 2012;79:216–25.
[19] Whittle JK, Williams MS, Karavasilis TL, Blakeborough A. A comparison of viscous damper placement methods for improving seismic building design. J Earthq Eng 2012;16:540–60.
[20] Soong TT, Grigoriu M. Random vibration of mechanical and structural systems. New Jersey: Prentice Hall; 1993.

[21] Vanmarcke EH. Structural response to earthquakes. In: Lomnitz C, Rosenblueth E, editors. Seismic risk and engineering decisions. Amsterdam: Elsevier; 1976.
[22] Giaralis A, Spanos PD. Effective linear damping and stiffness coefficients of non-linear systems for design spectrum based analysis. Soil Dyn Earthq Eng 2010;30:798–810.
[23] Clough RW, Penzien J. Dynamics of structures. 2nd ed.New York: Mc-Graw Hill; 1993.
[24] De la Fuente E. An efficient procedure to obtain exact solutions in random vibration analysis of linear structures. Eng Struct 2008;30:2981–90.
[25] I.B.C. International Building Code; 2003.
[26] Der Kiureghian A. Structural response to stationary excitation. J Eng Mech Div ASCE 1980;106:1195–213.
[27] Arora JS. Introduction to optimum design. 2nd ed.San Diego: Elsevier Ltd.; 2004.
[28] Belegundu AD, Chandrupatla TR. Optimization concepts and applications in engineering. 2nd ed.New York: Cambridge University Press; 2011.
[29] U.B.C. Uniform Building Code. vol. 1–3; 1997.
[30] Paz M. International handbook of earthquake engineering. Codes, programs, and examples, first ed. New York: Chapman & Hall; 1994.